Merve Nur Öztürk	Atakan Süslü	Betül Rana Kuran
2311322	*2311371*	*2311173*

1   Introduction

Numerical methods, such as Runge Kutta Method, are widely used to solve differential equations when an analytical solution is not possible or time-consuming. 4th order Runge-Kutta Method is one of the numerical methods which gives quite accurate results due to its small truncation error. In this homework, a solid propellant rocket is given, and its chamber pressure p_c, burn rate $\dot{r}$, and the specific impulse I_{sp} are asked to be calculated with this method until the chamber pressure p_c becomes equal to the atmospheric pressure p_a, with different time step sizes and different nozzle throat radiuses.

This equation gives the rate of the chamber pressure of the given rocket with a constant burn temperature T_c:

$$\frac{dp_c}{dt} = \frac{RT_c}{V_c}(\dot{m_{bs}} - \dot{m_{ce}} - \rho_c \dot{V_c}) \tag{1}$$

It is assumed that the propellant inner surface is circular and between the chamber exit and nozzle throat, no gas mass accumulates ($\dot{m_{ce}} = \dot{m_n}$). Moreover, writing $\dot{m_{bs}} = \rho_p 2\pi r L \dot{r}$, and $V_c = \pi r^2 L$, the equation becomes:

$$\frac{dp_c}{dt} = RT_c[\frac{2\dot{r}}{r}(\rho_p - \rho_c) - \frac{\dot{m_n}}{\pi r^2 L}] \tag{2}$$

It is given that $\dot{r} = ap_c^n$, and $\dot{m_n} = p_c A^* \sqrt{\frac{\gamma}{RT_c}}(\frac{\gamma+1}{2})^{-\frac{\gamma+1}{2(\gamma-1)}}$ where A^* is the nozzle throat area. Furthermore, though at first it was assumed that the propellant inner surface is circular, it is more of a complex shape. Thus, a propellant design dependent factor $f_{cor}(r)$ is used to simply approach to original characteristics. Then, the equations for the rate of chamber pressure, and the rate of equivalent radius r become:

$$\boxed{\frac{dp_c}{dt} = RT_c[f_{cor}(r)\frac{2ap_c^n}{r}(\rho_p - \frac{p_c}{RT_c}) - \frac{p_c A^*}{\pi r^2 L}\sqrt{\frac{\gamma}{RT_c}}(\frac{\gamma+1}{2})^{-\frac{\gamma+1}{2(\gamma-1)}}]} \tag{3}$$

$$\boxed{\frac{dr}{dt} = ap_c^n} \tag{4}$$

Specific impulse is also asked to be calculated, and its formula is:

$$\boxed{I_{sp} = \frac{1}{g}\sqrt{\frac{2\gamma RT_c}{\gamma - 1}[1 - (\frac{p_a}{p_c})^{\frac{\gamma-1}{\gamma}}]}} \tag{5}$$

2 Method

2.1 Classical Fourth-order RK Method

The basic form of the RK method is :

$$y_{i+1} = y_i + \Phi(x_i, y_i, \Delta x)\Delta x \tag{6}$$

Φ can be defined as a weighted slope function or increment function. It can be expressed as:

$$\Phi = a_1 k_1 + a_2 k_2 + ... + a_n k_n \tag{7}$$

where $k_1, k_2, ..., k_n$ are slopes, $a_1, a_2, ..., a_n$ are weights.
In classical fourth-order RK method, four slopes are calculated for each interval. Also, weights are equal to $1/6, 1/3, 1/3, 1/6$, respectively. In the homework, there is the system of ordinary differential equations, $\frac{dy_i}{dt}$ and $\frac{dr_i}{dt}$. Therefore, the RK method becomes:

$$
\begin{aligned}
y_{1,i+1} &= y_{1,i} + \frac{1}{6}(k_{1,1} + 2k_{2,1} + 2k_{3,1} + k_{4,1})\Delta x \\
y_{2,i+1} &= y_{2,i} + \frac{1}{6}(k_{1,2} + 2k_{2,2} + 2k_{3,2} + k_{4,2})\Delta x \\
\text{Stage 1: } k_{1,1} &= f_1(x_i, y_{1,i}, y_{2,i}) \\
k_{1,2} &= f_2(x_i, y_{1,i}, y_{2,i}) \\
y_1^* &= y_{1,i} + k_{1,1}(p_1\Delta x) \\
y_2^* &= y_{2,i} + k_{1,2}(p_1\Delta x) \\
\text{Stage 2: } k_{2,1} &= f_1(x_{i+(p_1\Delta x)}, y_1^*, y_2^*) \\
k_{2,2} &= f_2(x_{i+(p_1\Delta x)}, y_1^*, y_2^*) \\
y_1^{**} &= y_{1,i} + k_{2,1}(p_2\Delta x) \\
y_2^{**} &= y_{2,i} + k_{2,2}(p_2\Delta x) \\
\text{Stage 3: } k_{3,1} &= f_1(x_{i+(p_2\Delta x)}, y_1^{**}, y_2^{**}) \\
k_{3,2} &= f_2(x_{i+(p_2\Delta x)}, y_1^{**}, y_2^{**}) \\
y_1^{***} &= y_{1,i} + k_{1,3}(p_3\Delta x) \\
y_2^{***} &= y_{2,i} + k_{2,3}(p_3\Delta x) \\
\text{Stage 4: } k_{4,1} &= f_1(x_{i+(p_1\Delta x)}, y_1^{***}, y_2^{***}) \\
k_{4,2} &= f_2(x_{i+(p_3\Delta x)}, y_1^{***}, y_2^{***})
\end{aligned}
$$

where $y\prime = f(x_i, y_i)$ and $p_1 = p_2 = 1/2$, $p_3 = 1$.
At every stage, first, the slope of r_i ($k_{n,1}$) and p_{c_i} ($k_{n,2}$) at p_n fraction of interval is calculated. Then, temporary $p_{c_{i+(p_n\Delta x)}}$ and $r_{i+(p_n\Delta x)}$ values are determined, which enables to calculate the next slopes p_{n+1} fraction of the same interval. After four stages, weighted slopes are determined. By substituting known variables into Equation 6, next values r_{i+1} and $p_{c_{i+1}}$ are calculated.

2.2 Adaptive Stepping

When there is a sudden change in a region, a small step size must be used to calculate this sudden change. But if this sudden change is in a small region and ODE changes linearly in other regions, a small time step size is not necessary for the linear region. If a constant small time step size is used, sudden changes can be calculated correctly but computational speed will be wasted for the linear region. Also, small step sizes cause an increase in the number of steps, which leads to a rise in the round off errors, whereas large step sizes cause larger truncation errors. In order to solve this problem, adaptive step size can be used such that step size is bigger in linear regions, and if there is a sudden change, step size gets smaller so that results can be calculated correctly. In adaptive step size control, first, the local truncation error, E_o, is calculated. In this homework, E_o is determined by using the difference between the RK4 method and the RK2 method.

$$E_o = \frac{y_{RK4} - y_{RK2}}{y_{RK4}} \tag{8}$$

After the local truncation error E_o is determined, the new time step can be calculated with

$$\Delta x_{new} = \Delta x_{old} \left| \frac{E_{allowed}}{E_o} \right|^{0.20} \tag{9}$$

where $E_{allowed}$ is the allowed percent error tolerance and equal to 0.0001 in this homework.

3   Results and Discussion

3.1   Calculation of p_c, $\dot{r}$ and I_{sp} with different time step sizes
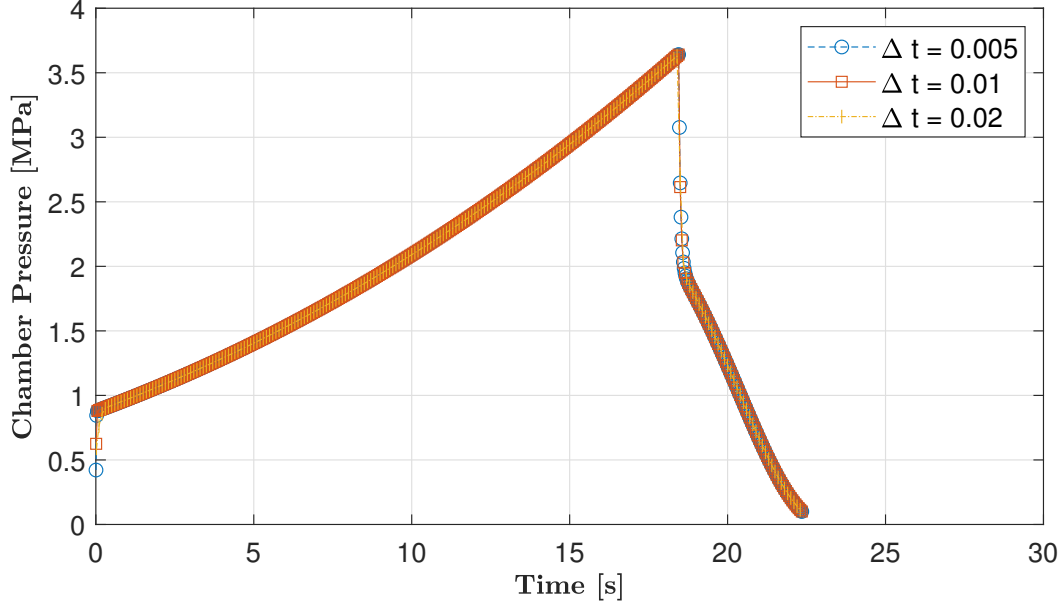

Figure 1: Calculated p_c values using 4th order RK method with three different step sizes.

This figure demonstrates how the chamber pressure p_c changes as time progresses. As can be seen in Figure 1, there are three curves, one for each step size. However, there is no significant difference between the curves, which results from the high degree of accuracy provided by the 4th order RK method. This is because the truncation error for this method is so small that its effect on the results can be nearly neglected. In addition, using smaller step sizes helps to calculate more precisely, and it is obvious that the step sizes used for this problem are small enough. As a result, the values obtained for the chamber pressure p_c of the rocket were approximately the same for three different step sizes.

Figure 2 and Figure 3 demonstrates the change in the rate of equivalent radius and the specific impulse with time, respectively. As it was for p_c, there are three curves also for the rate of the equivalent radius $\dot{r}$ in Figure 2 and the specific impulse I_{sp} in Figure 3. Since the conditions are the same as mentioned above, the values calculated for $\dot{r}$ and I_{sp} does not experience a major change for different step sizes. The point is, the accuracy of the results obtained by using the RK4 Method is remarkably of a high degree for the step sizes used in this problem.
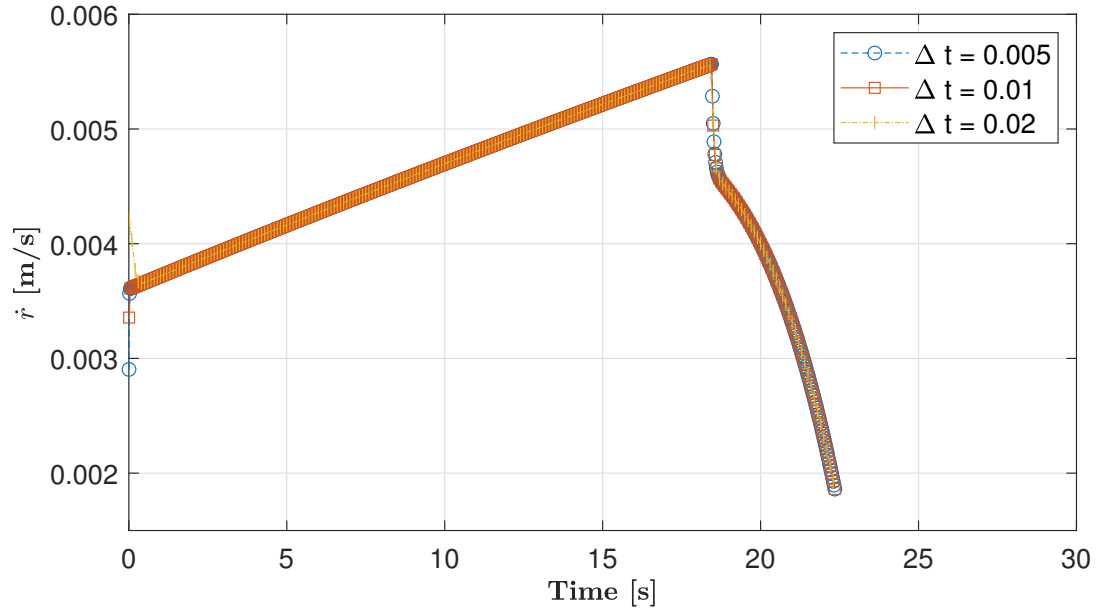
4

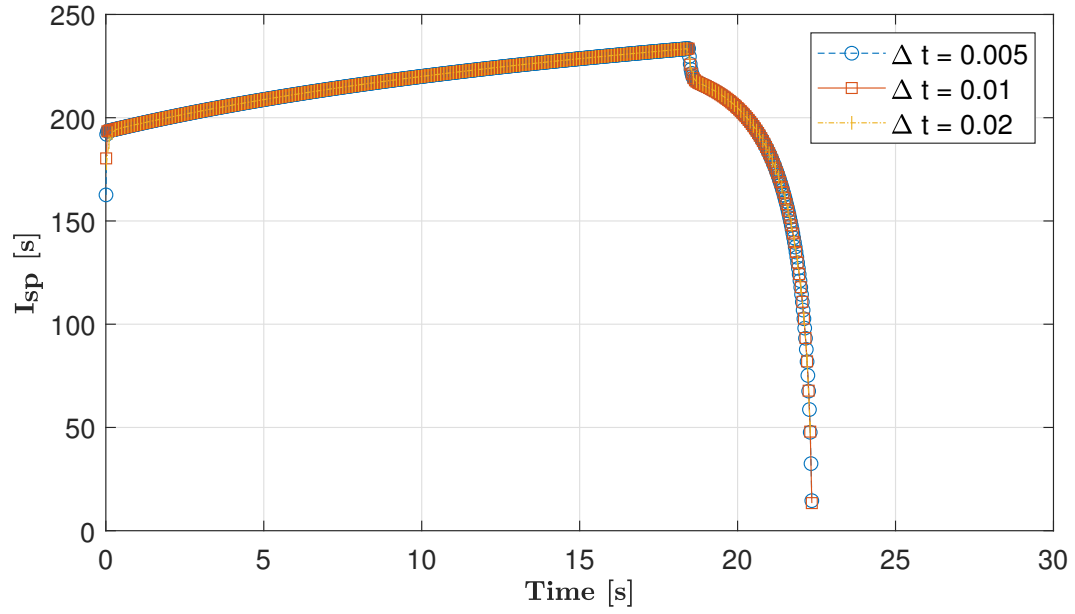Figure 2: Calculated $\dot{r}$ values using 4th order RK method with three different step sizes.

Figure 3: Calculated I_{sp} values using 4th order RK method with three different step sizes.

3.2 Calculation of p_c, $\dot{r}$ and I_{sp} with different nozzle throat radiuses
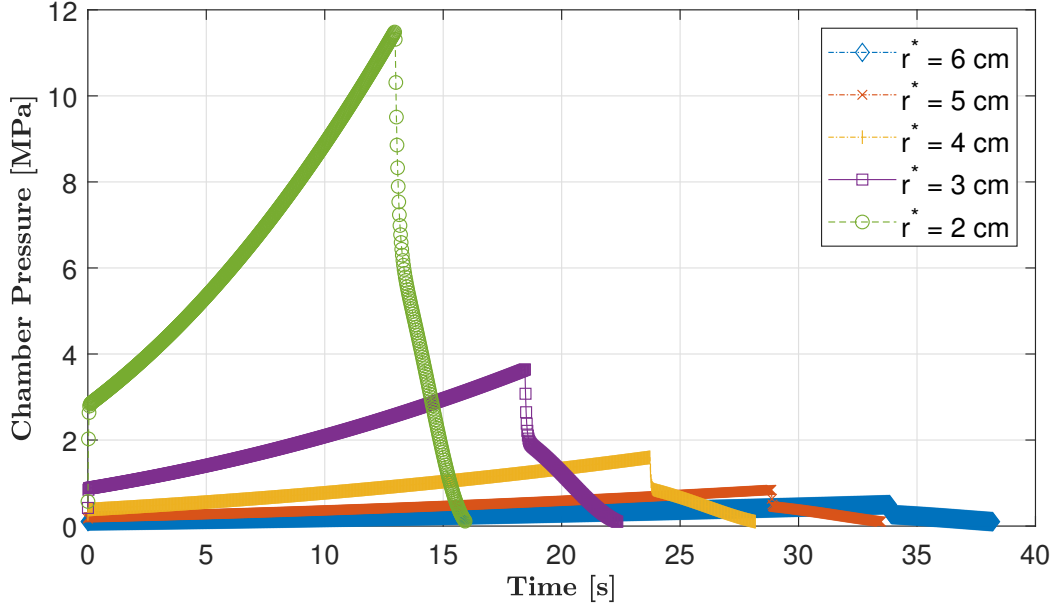

Figure 4: Calculated p_c values using 4th order RK method with different nozzle throat radiuses.

This figure demonstrates how the chamber pressure p_c changes as time progresses with different nozzle throat radiuses. As can be concluded from Figure 4, decreasing the radius of the nozzle throat leads to an increase in maximum chamber pressure and reduces the time needed for the chamber pressure to reach the ambient pressure. The reason of this is reducing the radius causes an exponential decrease in the area of the nozzle. As the area of the nozzle decreases, mass flowing out from the nozzle decreases, and total gas mass inside the cavity increases. This results in increased pressure inside the chamber. As the pressure increases, the propellant burns faster. Therefore, with a lower nozzle throat radius, propellant depletes faster resulting in shorter flight time.
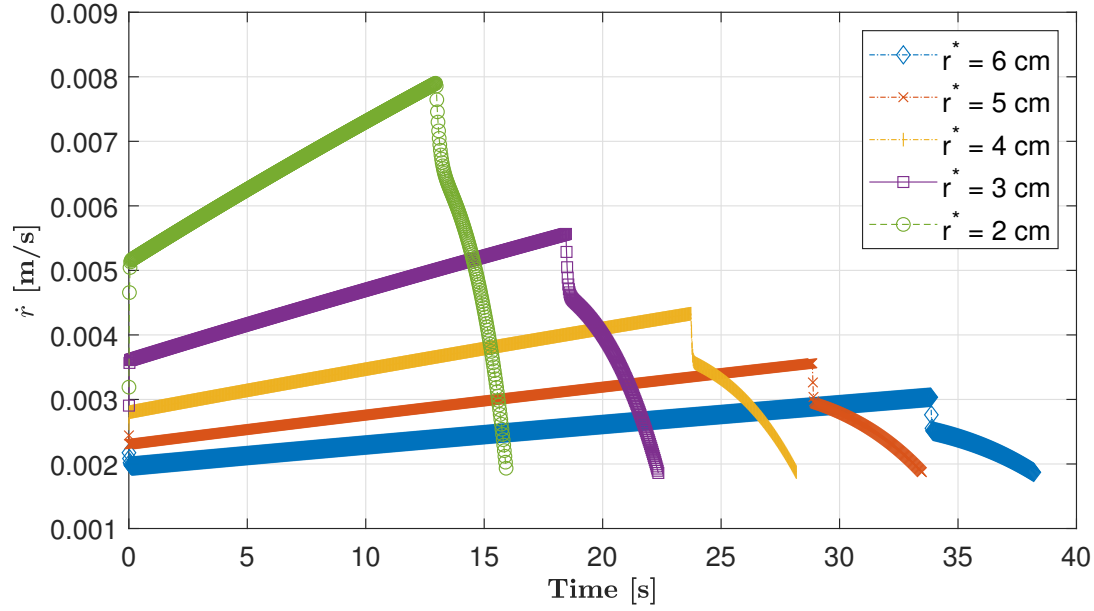
Figure 5: Calculated $\dot{r}$ values using 4th order RK method with different nozzle throat radiuses.

This figure illustrates how the burn rate $\dot{r}$ changes as time progresses with different nozzle throat radiuses. $\dot{r}$ is proportional to p_c as stated in Equation 4; therefore, both of them give similar responses to different throat radiuses. Lower radiuses cause higher maximum burn rates but shorter time to reach the ambient pressure. However, since the propellant burn rate exponent in Equation 4 is smaller than one, the growth in the maximum burn rates in Figure 5 is less remarkable than the growth in the maximum chamber pressures in Figure 4. Also, as mentioned above, flight time decreases because of a faster burn rate.
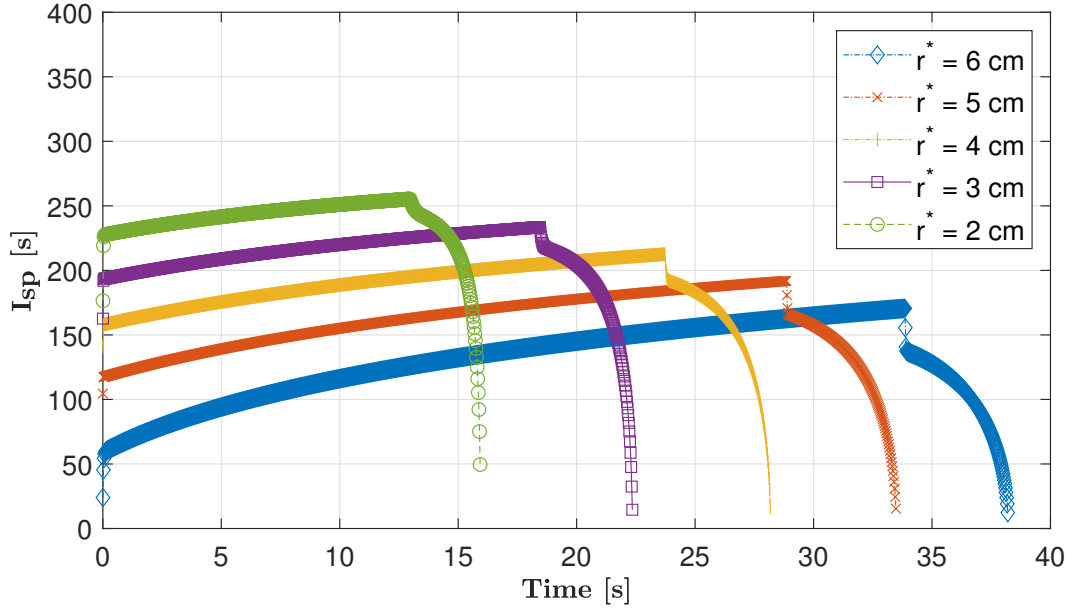
Figure 6: Calculated I_{sp} values using 4th order RK method with different nozzle throat radiuses.

This figure shows how the specific impulse I_{sp} changes as time progresses with different nozzle throat radiuses. Specific impulse is a function of chamber pressure p_c as stated in Equation 5. Therefore, it is not surprising to observe that the specific impulse gives similar reactions in Figure 6 as the chamber pressure gave in Figure 4 in terms of relationship with increasing nozzle throat radius. As the radius of the nozzle throat decreases, specific impulse also increases but flight time decreases. Thus, the lowest nozzle throat radius of 2 centimeters is the most efficient, as it has the highest specific impulse.

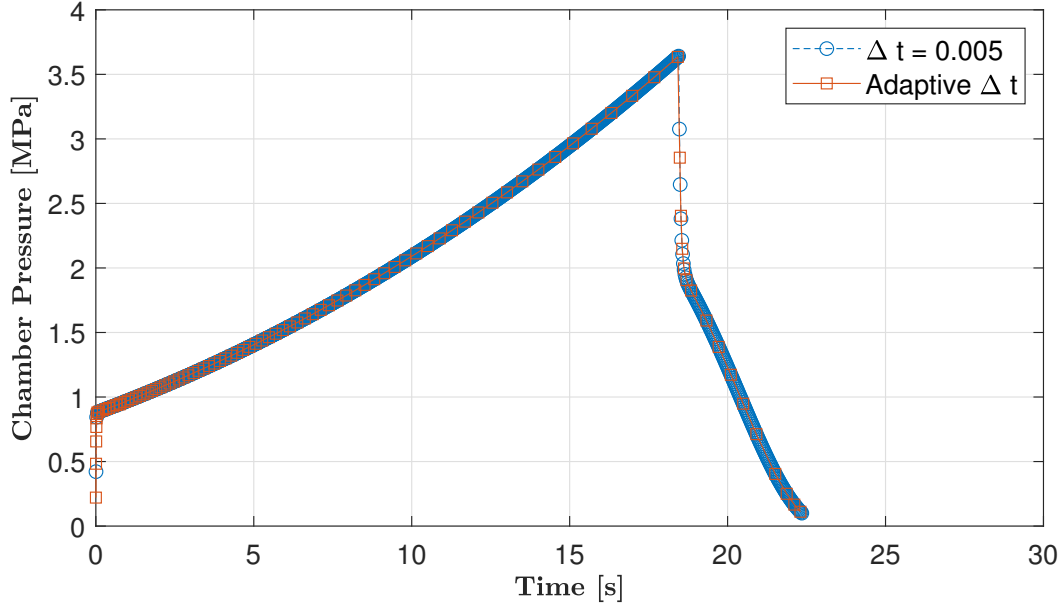## 3.3 Calculation of p_c, $\dot{r}$ and I_{sp} with adaptive stepping

Figure 7: Chamber pressure versus time graph with constant and adaptive step size.

Figure 7, Figure 8, and Figure 9 illustrate how the chamber pressure, the burn rate and specific impulse change as time progresses, respectively, using constant and adaptive time step sizes. It can be seen from Figures 7, 9, and 8 that when adaptive stepping is applied with allowed percent tolerance $E_o = 0.0001$, linear parts can be calculated with fewer steps without losing any accuracy as discussed in Section 2.2. When there is a sudden change, step size gets smaller accordingly and results can be calculated correctly in that region.

It can be seen from Table 1 that using adaptive stepping reduces the total number of time intervals needed significantly. Although results are calculated three times for each time interval(twice for determining the step size and once for calculating result) using the adaptive stepping approach, the number of time intervals needed is much lower than the constant step size approach. Therefore adaptive stepping is computationally cheaper without losing accuracy.

Table 1: Total number of time intervals needed for computations.

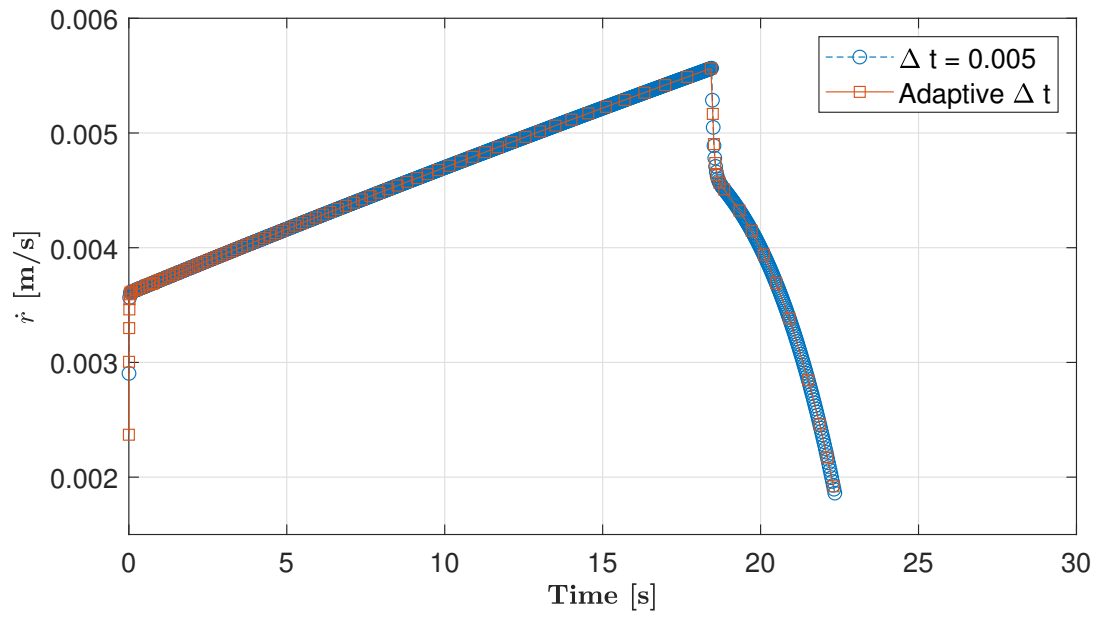| Stepping Approach	Number of time intervals needed
Constant $\Delta t = 0.005$	4470
Adaptive Stepping with initial $\Delta t = 0.005$	462

9

Figure 8: Burn rate versus time graph with constant and adaptive step size.
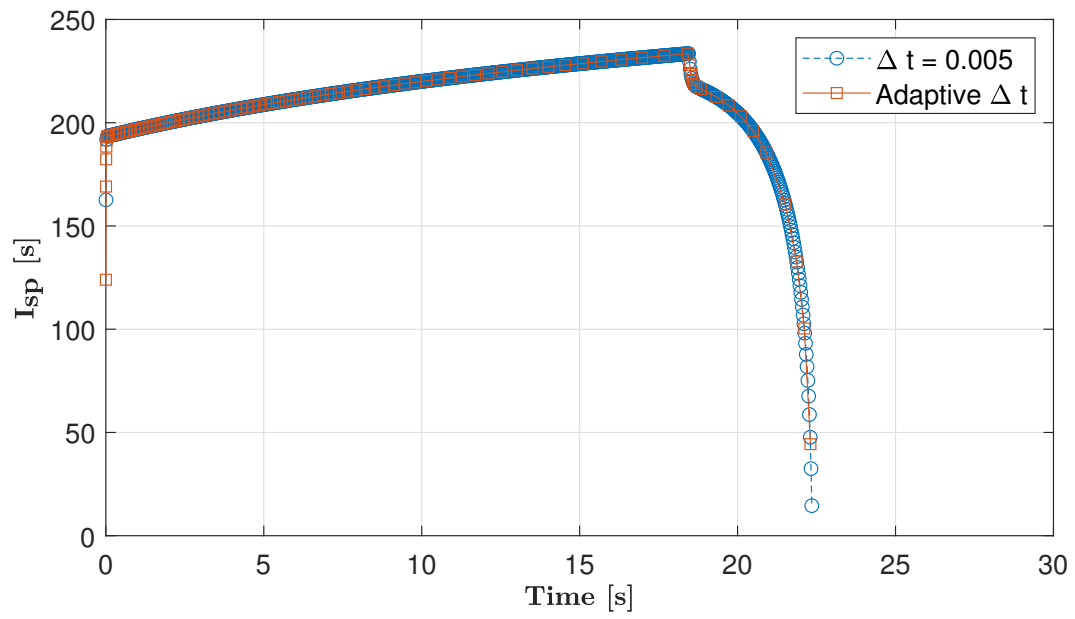

Figure 9: Specific impulse versus time graph with constant and adaptive step size.

4 Conclusion

Given a solid-propellant rocket, the change of chamber pressure p_c, the rate of the equivalent radius $\dot{r}$, and the specific impulse I_{sp} were requested to be calculated in the homework. These calculations were made by using the classical 4th order RK method with three different step sizes for the first problem, and with different nozzle throat radiuses for the second problem.

At first, comparing the results obtained, it can be observed that the 4th order RK method gives quite reliable results for this problem since the step sizes used are small enough to give minor error between solutions with different step sizes, and the truncation error caused by numerical methods is negligible for the 4th order RK method. Moving on to the next comparison, the results illustrate that the outcome of the usage of smaller nozzle throat radiuses is an increase in maximum chamber pressure. As the burn rate and the specific impulse are related proportionally to the chamber pressure, their maximum values also experience an increase. The smaller the nozzle throat radius the harder the gas flows out from the chamber and the pressure inside the chamber increases, which accounts for the increase in the values mentioned before.

As a final comment on the problem, it was demonstrated that the effect of adaptive stepping on the number of time intervals needed is extremely remarkable. It helps to increase the calculation speed without any loss of accuracy by using a smaller step size for sudden changes and a bigger step size for linear regions.